JOURNAL OF GUIDANCE, CONTROL, AND DYNAMICS
Vol. 20, No. 1, January–February 1997

Flight Control System Design with Rate Saturating Actuators

R. A. Hess* and S. A. Snell†
University of California, Davis, Davis, California 95616

Actuator rate saturation is an important factor adversely affecting the stability and performance of aircraft flight control systems. It has been identified as a catalyst in pilot-induced oscillations, some of which have been catastrophic. A simple design technique is described that utilizes software rate limiters to improve the performance of control systems operating in the presence of actuator rate saturation. As described, the technique requires control effectors to be ganged such that any effector is driven by only a single compensated error signal. Using an analysis of the steady-state behavior of the system, requirements are placed upon the type of the loop transmissions and compensators in the proposed technique. Application of the technique to the design of a multi-input/multi-output, lateral-directional control system for a simple model of a high-performance fighter is demonstrated as are the stability and performance improvements that can accrue with the technique.

I. Introduction

THE performance requirements of modern, high-performance, fly-by-wire aircraft have made it imperative that the characteristics of the actuation devices be included in any control system design procedure. For example, in the control of supermaneuverable aircraft, the reality of control actuator limitations can determine the overall control system design philosophy.[1] Although the linear dynamics of the actuator are often modeled in such designs, the nonlinear behavior, e.g., saturation, is not often considered in explicit fashion. Typically, extensive a posteriori simulation is employed to determine if and when actuator saturation is likely to occur and then if such saturation can affect flight safety. Even time-consuming simulation efforts are often unable to uncover situations that can affect flight safety. For example, probably no aircraft in the history of aviation has undergone more simulator evaluation than the Shuttle Orbiter. Yet a serious pilot-induced oscillation (PIO) occurred in early free-flight testing,[2] which led to actuator rate saturation. Actuator rate saturation has also been implicated in the YF-22 crash early in 1992 (Ref. 3) and possibly in the JAS 39 crash of 1993 (Ref. 4), both of which also experienced serious PIOs. Indeed, the pivotal role that actuator rate saturation may play in PIOs is coming under increased scrutiny.[5]

II. Background

Feedback design techniques that explicitly consider the possibility of control saturation are receiving increasing attention in the literature. Optimal control strategies for regulators employing inequality constraints on control and state variables are well known.[6] Techniques that attempt to minimize the adverse effects of saturation are also well established, e.g., antiwindup controllers.[7] Feedback systems designed to avoid saturation have been discussed.[8] Nonlinear feedback controllers designed with the goal of improved performance with state and control saturation have also been described.[9] Linear feedback schemes to improve the performance of systems with saturation nonlinearities have been formulated.[10] Finally, an alternate control scheme has been recently proposed to reduce the adverse effects of time delays associated with flight control system actuator rate limiting, particularly that which occurs in pilot-induced oscillations.[5,11]

As opposed to the methods just mentioned, the research to be described employs a technique for addressing actuator rate saturation that is very simple in theory and implementation. Closed-loop stability and performance are improved through the introduction of software rate limits, i.e., nonlinear systems that ensure that no rate commands are sent to the actuators that are beyond the capabilities of these devices. Software rate limits are certainly not novel; however, it is believed the technique to be described uses them in a unique manner. As will be seen, although the proposed design technique is very simple, it does require a particular feedback topology for its implementation.

Section III introduces the technique using a single-input/single-output (SISO) formulation and example. Section IV extends the technique to multi-input/multi-output (MIMO) designs and demonstrates the aforementioned limitations on feedback topology. This section also applies the technique to a lateral-directional flight control problem using a simple model of a high-performance fighter aircraft. Finally, a brief discussion of the design technique is presented in Sec. V, and conclusions are drawn in Sec. VI.

III. Software Rate Limits: SISO Systems

Software Limiter

Consider Fig. 1a, which shows a very simple SISO control system. Although the linear actuator dynamics are ignored here, it will be assumed that actuator rate limiting does occur. The rate limited actuator A_{RL} is modeled as shown in Fig. 1b. Figure 2 shows the proposed software limiter S_{RL} as part of a SISO feedback system. S_{RL} consists of a derivative element, followed by an amplitude limiter, followed by an integration element. As is evident from their structures, the input-output behavior of S_{RL} and A_{RL} (or an actual rate-limiting actuator) will be different. The former device employs no internal feedback, whereas the latter does. Consider the behavior of each element in isolation as shown in Fig. 3. The input is a ramp followed by a constant value. Although both elements result in

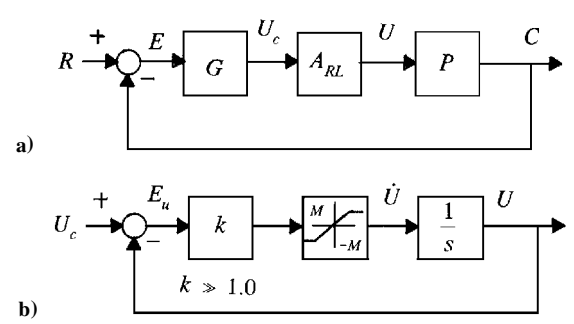

Fig. 1 Rate limiting in a control system: a) simple SISO system and b) the rate limiter A_{RL}.

Received Feb. 12, 1996; revision received Aug. 6, 1996; accepted for publication Oct. 18, 1996.

*Professor, Department of Mechanical and Aeronautical Engineering. Associate Fellow AIAA.

†Assistant Professor, Department of Mechanical and Aeronautical Engineering. Member AIAA.

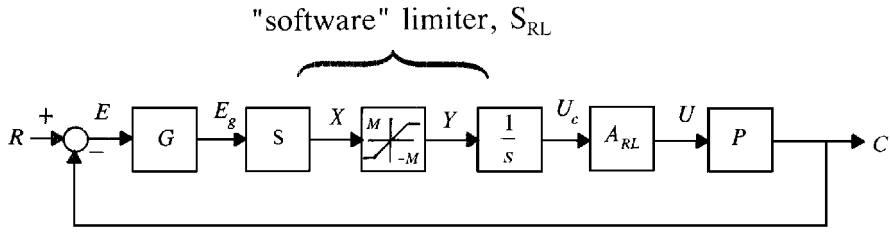

Fig. 2 System of Fig. 1a with a software rate limiter.

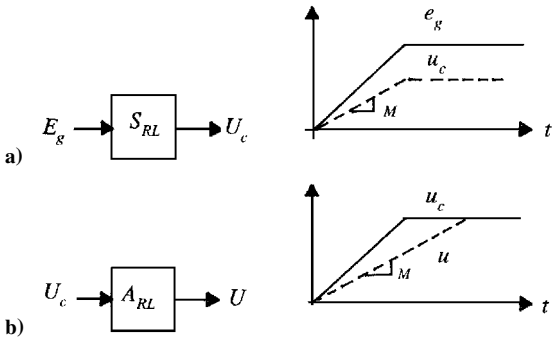

Fig. 3 Rate limiting behavior: a) input/output behavior of software limiter of Fig. 2 and b) input/output behavior of rate limiter of Figs. 1 and 2.

rate limited outputs, these outputs are quite different. The software limiter in Fig. 3a merely prevents rates beyond a certain magnitude from being sent to the actuator. It comes out of saturation as soon as $|\dot{x}(t)| < M$. The output of the rate limit element of Fig. 1b (and a rate limiting actuator) stays in saturation until the displacement error signal E_U becomes appropriately small. It is this latter behavior that can seriously compromise performance and stability when the actuator is part of a closed-loop system. As will be seen, the performance of a system with the software limiter and a rate-limiting actuator can be far superior to a system without the software limiter. However, the behavior of the software limiter leads to requirements upon the system loop transmission if steady-state performance is to be maintained. This will be demonstrated in the next section.

Quasilinear System and Steady-State Error

Consider Fig. 4, a quasilinear representation of Fig. 2, in which the limiter has been replaced by a remnant signal $d(t)$. The remnant is defined simply as that signal that must be added to $x(t)$ in Fig. 4 so that $y(t)$ in Fig. 4 is identical to $y(t)$ in Fig. 2 when limiting occurs. In what follows, the dynamics of the rate limiter A_{RL} can be neglected, because saturation of A_{RL} will be eliminated by S_{RL} and the linear dynamics of A_{RL} are negligible ($k \gg 1$ in Fig. 1b). Block diagram algebra can then be used to show the following:

$$Y = D + sGR - (sGPY/s) = D + sGR - LY \tag{1a}$$

$$(1 + L)Y = D + sGR \tag{1b}$$

$$D/(1 + L) \triangleq D_n = Y - [sGR/(1 + L)] = Y - Y_L \tag{1c}$$

where Y_L is the signal that would exist in either Fig. 2 or Fig. 4 when no limiting occurs. Note from Eq. (1) that D_n is merely the difference between Y (with limiting) and Y_L.

Now, from Fig. 4

$$E = [R/(1 + L)] - (D_n P/s) \tag{2}$$

A fundamental assumption in this analysis is that the closed-loop system of Fig. 2 is stable, even in saturation. This will allow the final value theorem to be applied to Eq. (2). Note that open-loop stability is not required, because if $P(s)$ has right half-plane poles, they will be canceled by identical poles of $D_n(s)$, a condition guaranteed by the assumption of closed-loop stability [$E(s)$ with no right half-plane poles]. Thus, invoking the final value theorem

$$e_{ss}(t) = \lim_{t \to \infty} e(t) = \lim_{s \to 0} sE \tag{3}$$

But, from Eq. (2),

$$sE = [sR/(1 + L)] - D_n P \tag{4}$$

Now denote the type of a transformed variable or transfer function A as q^A. Type refers to the exponent on any free s in the denominator of the transformed variable or transfer function.[12] Then the types of the first and second terms on the right-hand side of Eq. (4) are

$$q^{\text{1st term}} = q^R - q^L - 1 \tag{5a}$$

$$q^{\text{2nd term}} = q^{D_n} + q^P \tag{5b}$$

where it has been assumed in obtaining Eq. (5a) that $q^L \geq 0$, a criterion invariably met in any satisfactory feedback design. Now, unfortunately, D_n cannot be treated like an independent disturbance as evident from Eq. (1c), i.e., it will be dependent on the characteristics of the system into which it is injected, e.g., the loop transmission L. If $q^L > q^P$, then a necessary and sufficient condition for the stable linear system of Fig. 2 to exhibit asymptotic stability in response to $d(t)$ is $q^{D_n} \leq -q^L$. A conservative expression for q^{D_n} could then be offered as

$$q^{D_n} = -q^L \tag{6}$$

Using Eq. (6), the right-hand side of Eqs. (5a) and (5b) will be negative and $e_{ss}(t) \to 0$ if

From Eq. (5a):

$$q^L \geq q^R \tag{7a}$$

From Eq. (5b):

$$q^L \geq q^P + 1 \qquad \text{or} \qquad q^G \geq 1 \tag{7b}$$

Although dependent on the assumption of stability, inequalities (7) provide design guidance and offer necessary conditions for asymptotic stability. The requirements implied by inequalities (7) are necessitated by the aforementioned behavior of the software limiter, i.e., $y(t)$ not approaching $x(t)$ after a period of limiting. In general, the larger the q^L, the better the performance of the system with the software limiter, provided that adequate stability margins can be maintained in the linear design.

SISO Example

Consider the system of Fig. 1. Let

$$P = \frac{1}{s} \qquad G = \frac{2}{0.05s + 1} \tag{8}$$

The compensator G has been designed so that the loop transmission has a crossover frequency of 2 rad/s, with desirable loop transmission characteristics. The amount of rate limiting will be adjusted to produce significant saturation in this example. Assuming that

$$q^R \leq 1 \tag{9}$$

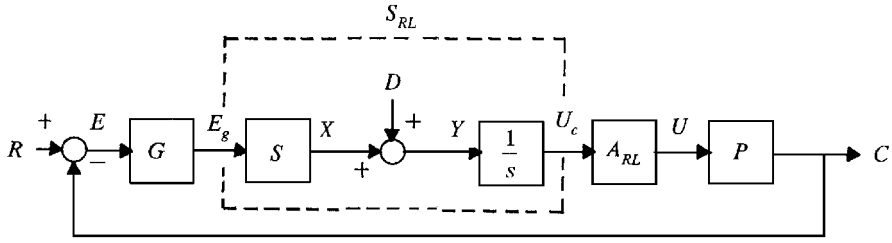

Fig. 4 Quasilinear representation of Fig. 2.

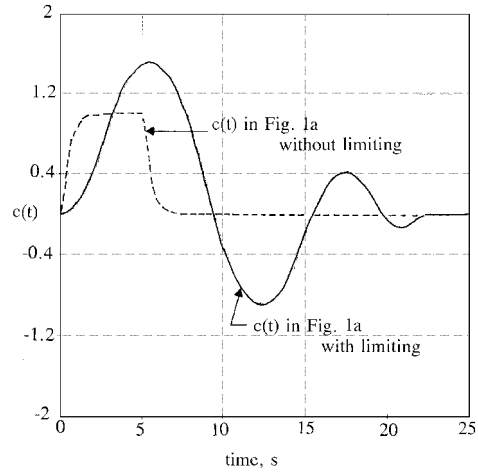

Fig. 5 Response of system of Fig. 1a to pulsive input, with and without rate saturation.

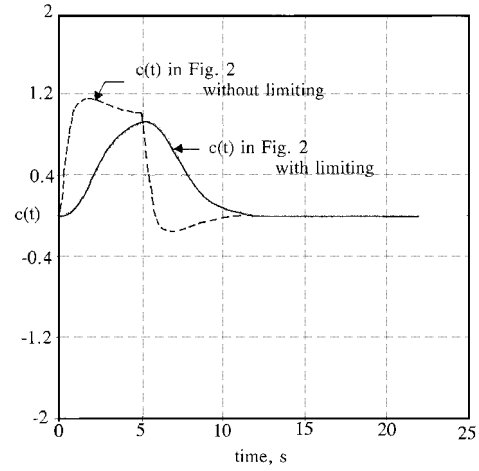

Fig. 6 Response of system of Fig. 2 to pulsive input, with and without rate saturation.

then inequalities (7) require that

$$q^L \geq q^p + 1 = 2 \tag{10}$$

Inequality (10) requires that the type of the loop transmission $L = GP$ be increased from the type 1 implied by Eq. (8) when the system of Fig. 2 is implemented. Thus, one can define a new compensator as

$$G' = G \cdot \frac{(s + 0.5)}{s} \tag{11}$$

This modification of the original compensator G will cause some change in the performance of the system of Fig. 2 as compared with that of the system of Fig. 1a when no saturation occurs; i.e., there will be a modest reduction in stability margins. Finally, the s appearing before the limiter in Fig. 2 will be included in the compensator in actual implementation. Although the resulting compensator sG' is now only proper, as opposed to being strictly proper, the integrator following the limiter will restore the latter property. This can be important from the standpoint of sensor noise propagation to the plant actuator.

Figure 5 shows the response of the system of Fig. 1a to a pulsive input of unity magnitude and 5-s duration with and without rate saturation. For the case with saturation, the rate limit was 0.2/s. Figure 6 shows the response of the system of Fig. 2 [with compensator $G'(s)$ and the software limiter] to the same input, with and without the rate limit of 0.2/s. The performance improvement with saturation is obvious. An examination of the actuator rate time histories in this example indicated that the system of Fig. 2 was in saturation far less than the system of Fig. 1a. A comparison of the dashed curves in Figs. 5 and 6 show that the performance of the system of Fig. 2 is somewhat poorer than that of Fig. 1a when no saturation occurs. This is attributable to a slight reduction in stability margins when q^L was increased from 1 to 2 [using $G'(s)$ as opposed to $G(s)$] as dictated by inequality (10). However, this is a small price to pay for the performance improvement that occurs with saturation.

Figure 7 compares the signals $u(t)$ for the systems of Figs. 1a and 2 when a sinusoidal input

$$r(t) = \sin(3t) \tag{12}$$

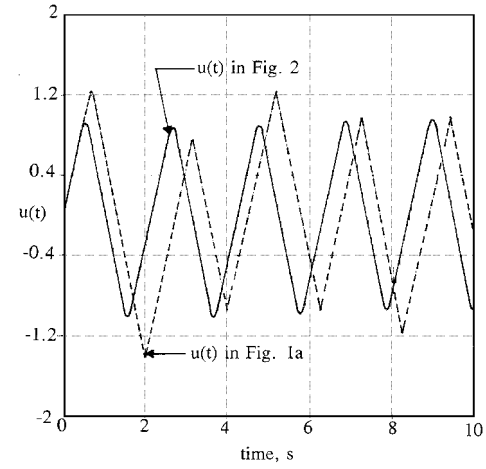

Fig. 7 Comparison of signals $u(t)$ in systems of Figs. 1a and 2 with sinusoidal input and rate saturation.

was applied. Here the rate limit was set to 2.0/s. The characteristics of $u(t)$ indicate that both systems were in nearly constant rate saturation of ± 2.0/s throughout. Because of this significant limiting, the tracking behavior of both the systems of Figs. 1a and 2 was poor. What is important, however, is the fact that the response $u(t)$ of Fig. 1a exhibits an effective incremental time delay of 0.55 s compared with the same system without rate limits. In comparison, the response $u(t)$ of Fig. 2 exhibits an effective incremental delay of only 0.12 s compared with the same system without rate limits. The effective incremental delays were calculated between corresponding instants when $\dot{u}(t)$ changes sign. If the systems of Figs. 1a and 2 were representing the stability and command augmentation system of an aircraft, with $r(t)$ being the pilot's input, the much larger delay of the system of Fig. 1a would probably lead to this system being more prone to PIOs than the system of Fig. 2 (Ref. 5).

IV. Software Rate Limits: MIMO Systems

Software Limiters

Any application of the technique introduced in Sec. III to a realistic aircraft flight control problem must allow consideration of

MIMO systems. This section is directed to that end. For purposes of exposition, a 2×2 system will be employed, i.e., two inputs and two controlled outputs. Figure 8a shows the nonlinear system, and Fig. 8b shows its quasilinear representation. Note that n_e control effectors are allowed (where n_e can be any number). However, the effectors must be ganged; i.e., a group of effectors or actuators is driven by only one of the n_r compensated error signals. Here $n_r = 2$. In this case, the ganging is done by matrix K, each row of which contains only one nonzero entry. These elements are numerically equal to the rate limit of the ith actuator. Thus, in Figs. 8a and 8b, none of the $\dot{\delta}_{c_i}$ will exceed the rate limits of the associated actuators. The K matrix can be succinctly expressed as

$$K = R_L \cdot \Gamma \tag{13}$$

where R_L is an $n_e \times n_e$ diagonal matrix with the actuator rate limits appearing along the diagonal and Γ is the $n_e \times n_r$ control distribution matrix. Each row of Γ contains only one nonzero element, which is unity. The justification for this choice of K will be presented in what follows.

In Figs. 8a and 8b, the dynamics of the actuators (with limiting) are assumed to be included in the plant element P_{ij}. Finally, one can define an effective plant matrix P_e as

$$P_e = P \cdot K \tag{14}$$

Quasilinear System and Steady-State Error

Following a procedure analogous to that which yielded Eqs. (1), D_{n_1} and D_{n_2} in Fig. 8b can be shown to be

$$D_{n_1} = D_1/(1+L_1) = Y_1 - Y_{1_L} \qquad D_{n_2} = D_2/(1+L_2) = Y_2 - Y_{2_L} \tag{15}$$

Each Y_{i_L} in Eqs. (15) can be defined as the signal Y_i that would exist if no rate limiting was occurring in the ith software limiter, alone. As Fig. 8a indicates, amplitude, as well as rate limiting, can occur in the control system actuators. However, the D_{n_i} in the quasilinear systems of Figs. 4 and 8b have been assumed to arise from software limiters alone. Thus, the effects of actuator amplitude limiting cannot be considered in this analysis.

The loop transmissions L_i obtained by successively opening the loops in Fig. 8b at U_{ci} are given as

$$L_1 = G_1 \cdot \frac{P_{e_{11}} + G_2\Delta}{1 + P_{e_{22}}G_2} \tag{16a}$$

$$L_2 = G_2 \cdot \frac{P_{e_{22}} + G_1\Delta}{1 + P_{e_{11}}G_1} \tag{16b}$$

where

$$\Delta = P_{e_{11}}P_{e_{22}} - P_{e_{12}}P_{e_{21}} \tag{16c}$$

By a procedure analogous to that used to obtain Eq. (4), one can show

$$sE_1 = \frac{sR_1}{1+L_1} - \frac{sP_{e_{12}}G_2R_2}{(1+L_1)\left(1+P_{e_{22}}G_2\right)} - \frac{D_{n_1}L_1}{G_1} - \frac{D_{n_2}P_{e_{12}}(1+L_2)}{(1+L_1)} \cdot \frac{1}{\left(1+P_{e_{22}}G_2\right)} \tag{17a}$$

$$sE_2 = \frac{sR_2}{1+L_2} - \frac{sP_{e_{21}}G_1R_1}{(1+L_2)\left(1+P_{e_{11}}G_1\right)} - \frac{D_{n_2}L_2}{G_2} - \frac{D_{n_1}P_{e_{21}}(1+L_1)}{(1+L_2)} \cdot \frac{1}{\left(1+P_{e_{11}}G_1\right)} \tag{17b}$$

Each of the four terms on the right-hand sides of Eqs. (17a) and (17b) represents contributions from the four exogenous inputs R_1, R_2, D_{n_1}, and D_{n_2} (remembering that D_{n_i} are not really exogenous).

Assuming that the closed-loop system of Fig. 8a is stable, even with saturation, the final value theorem can be invoked as with the previous SISO system. As was done in Eqs. (5), one can determine the type of each of the terms on the right-hand side of Eqs. (17a) and (17b) as follows.

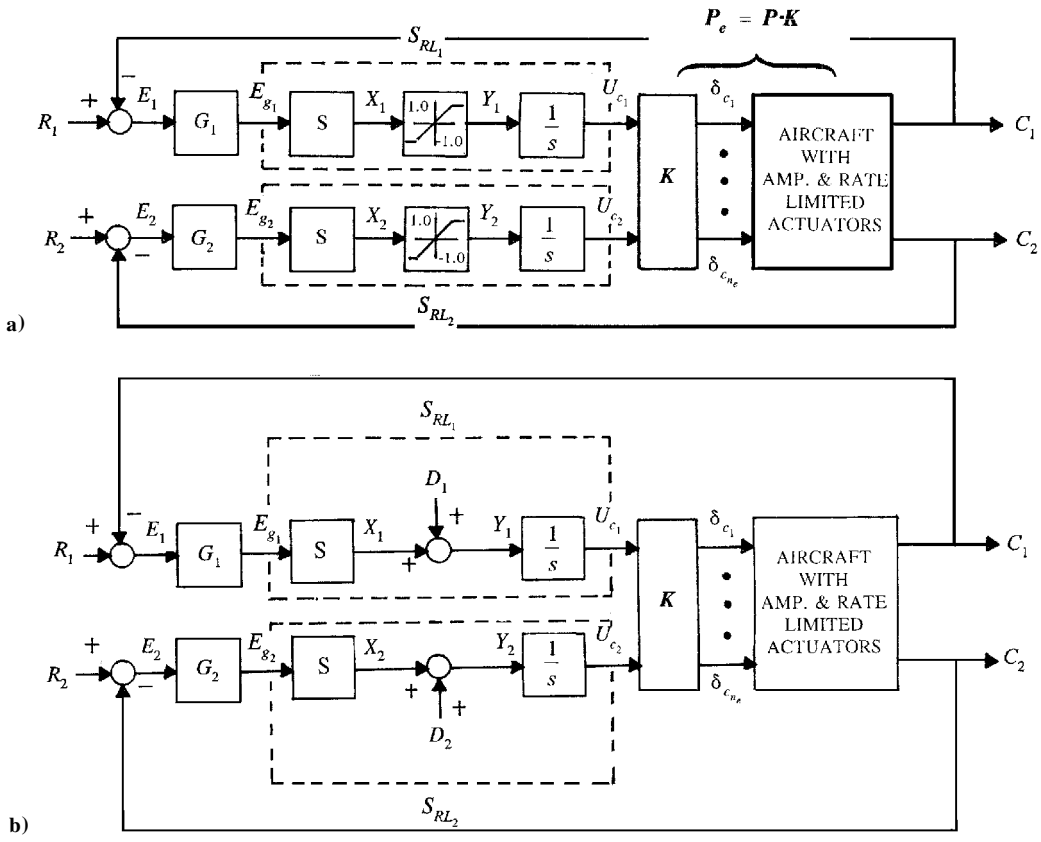

Fig. 8 A 2×2 MIMO system: a) with software rate limiting and b) a quasilinear representation of panel a.

Equation (17a):

$$\begin{aligned} q^{1\text{st term}} &= q^{R_1} - q^{L_1} - 1 \\ q^{2\text{nd term}} &= q^{R_2} + q^{P_{e_{12}}} - q^{L_1} - q^{P_{e_{22}}} - 1 \\ q^{3\text{rd term}} &= q^{D_{n_1}} + q^{L_1} - q^{G_1} \\ q^{4\text{th term}} &= q^{D_{n_2}} + q^{P_{e_{12}}} - q^{L_1} + q^{L_2} - q^{P_{e_{22}}} - q^{G_2} \end{aligned} \tag{18}$$

Equation (17b):

$$\begin{aligned} q^{1\text{st term}} &= q^{R_2} - q^{L_2} - 1 \\ q^{2\text{nd term}} &= q^{R_1} + q^{P_{e_{21}}} - q^{L_2} - q^{P_{e_{11}}} - 1 \\ q^{3\text{rd term}} &= q^{D_{n_2}} + q^{L_2} - q^{G_2} \\ q^{4\text{th term}} &= q^{D_{n_1}} + q^{P_{e_{21}}} - q^{L_2} + q^{L_1} - q^{P_{e_{11}}} - q^{G_1} \end{aligned} \tag{19}$$

In obtaining Eqs. (18) and (19) it has been assumed that $q^{L_i} \geq 0$ and $q^{P_{e_{ii}} G_i} \geq 0$, criteria invariably met in the satisfactory design of the feedback system of Fig. 8a. The design task is to select q^{L_i} and $q^{G_i} (i = 1, 2)$ so that

$$q^{j\text{th term}} \leq -1 \qquad (j = 1, 2, \ldots) \tag{20}$$

in Eqs. (18) and (19). As in Eqs. (6) and (9), allowing

$$q^{D_{n_i}} = -q^{L_i} \qquad q^{R_i} \leq 1 \tag{21}$$

Eqs. (20) and (21) lead to Eqs. (18) and (19) requiring

$$\begin{gathered} q^{L_1} \geq 1 \qquad q^{L_1} \geq q^{P_{e_{12}}} - q^{P_{e_{22}}} + 1 \qquad q^{G_1} \geq 1 \\ q^{L_1} \geq q^{P_{e_{12}}} - q^{P_{e_{22}}} - q^{G_2} + 1 \end{gathered} \tag{22}$$

and

$$\begin{gathered} q^{L_2} \geq 1 \qquad q^{L_2} \geq q^{P_{e_{21}}} - q^{P_{e_{11}}} + 1 \qquad q^{G_2} \geq 1 \\ q^{L_2} \geq q^{P_{e_{21}}} - q^{P_{e_{11}}} - q^{G_1} + 1 \end{gathered} \tag{23}$$

The final value theorem and inequality (20) will ensure

$$e_{i_{ss}}(t) = 0 \qquad i = 1, 2 \tag{24}$$

The q^{L_i} are governed by the q^{G_i} as evident in Eqs. (16a) and (16b). Of course, the methodology just outlined can be extended to 3×3, 4×4 systems, etc. As in the case of the SISO design, open-loop stability is not required.

Ganged Controls

The explanation for imposing ganged controls can now be given. First, grouping each software limiter with a compensator ensures that the type of each of the n_r loop transmissions q^{L_i} (n_r = number of controlled outputs) can be determined by a single compensator; e.g., in Eq. (16), q^{L_1} can be governed by G_1, etc. Second, ganging the effectors and defining the nonzero elements of the K matrix as in Eq. (13) allows n_r software limiters to prevent rate saturation of n_e actuators, with $n_e > n_r$.

MIMO Example

The aircraft example to be examined involves the lateral-directional control of a model of a high-performance fighter aircraft. The simplified aircraft and actuator dynamics were taken from Ref. 13 and are repeated here in Table 1. Rather than employing the simple rate limiter shown in Fig. 1b, a more accurate representation of a rate and amplitude limited second-order actuator was employed. This actuator model is shown in Fig. 9 (Ref. 14). The controlled outputs are sideslip β and roll rate $p_s(t)$ about the x stability axis. Note here that $n_r = 2$ and $n_e = 5$. Thus, in terms of Fig. 8b, $R_1 = \beta_c F_\beta$, $C_1 = \beta$, $R_2 = p_c F_p$, $C_2 = p_s$, $G_1 = G_\beta$, and $G_2 = G_p$. Selection of which of the five control effectors to associate with each of the compensators can be based upon the control axis authority of the effectors themselves. Here, for example, the rudder input δ_R and yaw

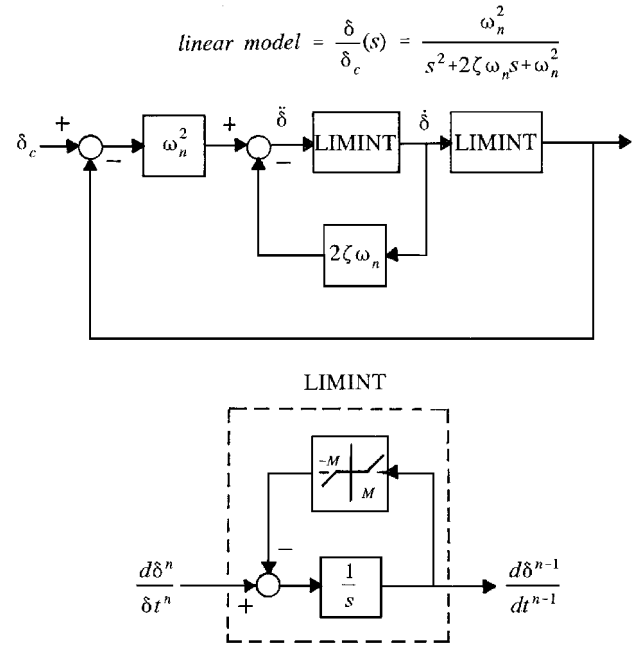

Fig. 9 Model of a second-order amplitude and rate limited actuator.

thrust vector input δ_{YTV} were used to control sideslip β, and the differential elevator input δ_{DT}, aileron input δ_A, and differential pitch thrust vector input δ_{RTV} were used to control roll rate p_s. Obviously, other choices could have been made. In terms of Eqs. (13),

$$R_L = \begin{bmatrix} 60 & 0 & 0 & 0 & 0 \\ 0 & 100 & 0 & 0 & 0 \\ 0 & 0 & 100 & 0 & 0 \\ 0 & 0 & 0 & 60 & 0 \\ 0 & 0 & 0 & 0 & 60 \end{bmatrix} \text{deg/s} \qquad \Gamma = \begin{bmatrix} 0 & 1 \\ 0 & 1 \\ 1 & 0 \\ 0 & 1 \\ 1 & 0 \end{bmatrix} \tag{25}$$

$$K = R_L \cdot \Gamma = \begin{bmatrix} 0 & 60 \\ 0 & 100 \\ 100 & 0 \\ 0 & 60 \\ 60 & 0 \end{bmatrix} \text{deg/s}$$

and

$$\delta = [\delta_{DT}, \delta_A, \delta_R, \delta_{RTV}, \delta_{YTV}]^T$$

A classical loop-shaping procedure was used to determine the compensators G_β and G_p, shown in Table 1. The crossover frequencies of each loop were selected as

$$\omega_{c_\beta} = 5.0 \text{ rad/s} \qquad \omega_{c_p} = 4.0 \text{ rad/s} \tag{26}$$

In this application, $q^{P_{e_{ij}}} = 0$, and inequalities (22) and (23) merely require that

$$q^{L_\beta} \geq 1, \qquad q^{L_p} \geq 1, \qquad q^{G_1} \geq 1, \qquad q^{G_2} \geq 1 \tag{27}$$

With the G_β and G_p of Table 1, inequalities (27) would already be met with $q^{L_\beta} = q^{L_p} = 1$. However, the types of G'_β and G'_p were chosen so as to yield

$$q^{L_\beta} = q^{L_p} = 2 \tag{28}$$

Thus,

$$G'_\beta = G_\beta \frac{(s + 0.5)}{s} \qquad G'_p = G_p \frac{(s + 0.4)}{s} \tag{29}$$

Table 1 Vehicle dynamics and compensation

Flight condition

Altitude = 20,000 ft, $M = 0.5$, $\alpha_{\text{trim}} = 5.4$ deg

Vehicle dynamics

$$\dot{\boldsymbol{x}} = \boldsymbol{A}x + \boldsymbol{B}\boldsymbol{u} \qquad \boldsymbol{X} = [\beta, p, r]^T$$

$$\boldsymbol{u} = [\delta_{DT}, \delta_A, \delta_R, \delta_{RTV}, \delta_{YTV}]^T$$

$$\boldsymbol{A} = \begin{bmatrix} -0.1354 & 0.09036 & -0.9949 \\ -10.37 & -1.469 & 0.5126 \\ 2.181 & -0.01482 & -0.1277 \end{bmatrix}$$

$$\boldsymbol{B} = \begin{bmatrix} -0.01091 & -0.005695 & 0.01555 & 0 & 0.00489 \\ 9.93 & 12.12 & 0.9416 & 0.3977 & 0.02817 \\ 0.2757 & -0.2797 & -0.7419 & -0.001175 & -0.3861 \end{bmatrix}$$

where

State variables

β = sideslip angle, deg
p = roll rate, deg/s
r = yaw rate, deg/s

Controlled responses variables

β = sideslip angle, deg
$p_s = \sin(\alpha_{\text{trim}})p + \cos(\alpha_{\text{trim}})r$, roll rate about x stability axis, deg/s

Control effectors

δ_{DT} = differential horizontal stabilizer, deg
δ_A = aileron, deg
δ_R = rudder, deg
δ_{RTV} = differential pitch thrust vectoring, deg
δ_{YYV} = yaw thrust vectoring, deg

Actuator dynamics

δ_{DT}:

$\dfrac{30^2}{[0.707, 30]}$ [a] rate limit = 60 deg/s ampl. limit = ±17.5 deg

δ_A:

$\dfrac{75^2}{[0.59, 75]}$ rate limit = 100 deg/s ampl. limit = ±27.5 deg

δ_R:

$\dfrac{72^2}{[0.69, 72]}$ rate limit = 100 deg/s ampl. limit = ±30.0 deg

δ_{RTV} and δ_{YTV}:

$\dfrac{20^2}{[0.6, 20]}$ rate limit = 60 deg/s ampl. limit = ±30.0 deg

Compensators[b]

$$G_\beta = \frac{42613(1)^2}{(0)(100)^2} \qquad G'_\beta = G_\beta \frac{(0.5)}{(0)}$$

$$G_p = \frac{22.8(2)}{(0)(100)} \qquad G'_p = G_p \frac{(0.4)}{(0)}$$

Prefilters

$$F_\beta = \frac{2^2}{[0.707, 2]} \qquad F_p = \frac{10^2}{[0.707, 10]}$$

[a] $\{K(z_1)/(p_1)[\zeta_1, \omega_1]\} = \{K(s + z_1)/(s + p_1)[s^2 + 2\zeta_1\omega_1 s + \omega_1^2]\}$.
[b] Compensator prior to inclusion of s before limiter.

Increasing the type q^{L_β} of q^{L_p} from 1 to 2 will improve the performance of the software limiters, provided, of course, that stability margins are not appreciably reduced by this increase, and they were not in this application. Note that the zeros in Eq. (29) were chosen to be a decade below the crossover frequencies of the associated loops so as to preserve the crossover characteristics of L_β and L_p. The final compensators are given in Table 1 along with the prefilter dynamics F_β and F_p. The bandwidths of the resulting closed-loop transfer functions, β/β_c and p_s/p_c, are determined by F_β and F_p. As in the case of the SISO example, in implementing the software limiters, the s appearing before each limiter was subsumed into the compensator that preceded it.

Figures 10 and 11 show the p_s and β responses with and without the software limiters to inputs defined as follows.

Figure 10:

$$\beta_c(t) = 0 \text{ deg} \qquad p_c(t) = 180 \cdot i(t) \text{ deg/s}$$

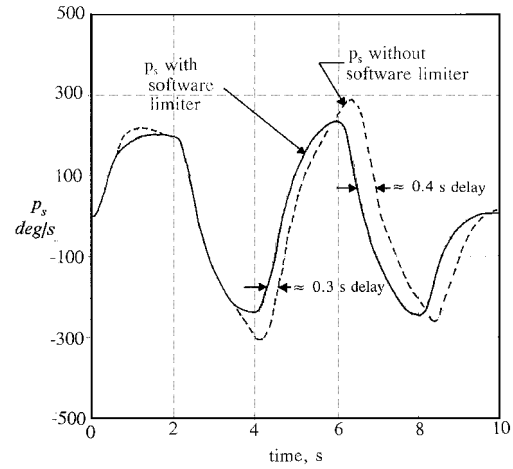

Fig. 10 Roll rate response of system of Fig. 8a to input of Eqs. (30), with and without software rate limiter (rate and amplitude limited actuators always present).

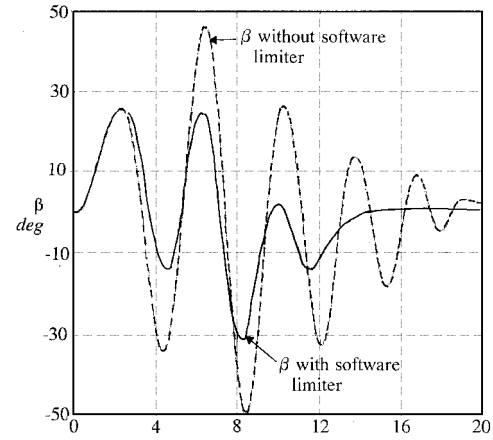

Fig. 11 Sideslip response of system of Fig. 8a to input of Eqs. (30) with and without software rate limiter (rate and amplitude limited actuators always present).

Figure 11:

$$\beta_c(t) = 30 \cdot i(t) \text{ deg} \qquad p_c(t) = 0 \text{ deg/s} \qquad (30)$$

where

$$i(t) = u(t) - 2u(t-2) + 2u(t-4) - 2u(t-6) + u(t-8)$$

and $u(t)$ = unit step.

As can be seen, the responses of the systems with software limiters are superior to those without. This is especially evident in the β responses. Although not as dramatic a difference exists between the p_s responses, the response of the system without the software limiters lags the response of the system with the limiters by as much as 0.3–0.4 s for $t > 4$ s. In terms of handling qualities degradations, effective time delay increments of these magnitudes are certainly very serious.[15] It should be emphasized that in the simulation the actuators themselves always contain the rate and amplitude limiters shown in Fig. 9 and Table 1, and actuator amplitude limiting did occur with and without the software limiters. In addition, of course, software rate limiting occurred when these limiters were in place, and actuator rate limiting occurred when they were not.

At the trim Mach number and altitude given in Table 1, the large roll rates in Fig. 10 do not necessarily invalidate the use of a linear aerodynamic model. However, the large sideslip angles in Fig. 11 for the system without software limiting are certainly in the nonlinear aerodynamic range. Bearing in mind that this example was not intended to serve as an accurate predictor of vehicle response in large amplitude maneuvers but to demonstrate the performance improvements that can accrue with the proposed design approach, the results demonstrated in Figs. 10 and 11 were deemed acceptable.

V. Discussion

The analyses of Secs. III and IV have always begun with the assumption of closed-loop stability. Then necessary and sufficient conditions for asymptotic stability were used to derive a relation between the type of the injected signals $D_{n_i}(s)$ in the quasilinear representation of the system and the type of the loop transmissions $L_i(s)$. Of course, stability under linear operation is guaranteed; however, stability under limiting conditions is not. This is especially true if open-loop stability is not in evidence. However, when saturation occurs, and closed-loop stability is in evidence, the proposed technique will always result in improved performance as compared with a system with a similar feedback topology in which it is not employed. Stability limitations under saturation still need to be determined through simulation.

Finally, it is imperative to point out that the rate limitations of flight control actuators are a function of aerodynamic loading. Thus, a practical implementation of the proposed design might require the elements of the K matrix in Eq. (14) and Fig. 8a to be scheduled with dynamic pressure.

VI. Conclusions

Based on the research just described, the following conclusions can be drawn.

1) The inclusion of very simple software rate limiters in a flight control system with appropriate compensator and loop transmission types may offer significant performance improvements in the presence of actuator rate saturation.

2) As presented here, the design technique requires control effectors to be ganged or grouped so that any effector or actuator is driven by a single compensated error signal.

3) The design technique places restrictions upon the type of the loop transmissions and compensators, where type refers to the exponent on any free s in the denominator of the transfer function.

4) An approach was offered for determining the restrictions upon the transfer function type by examination of the steady-state behavior of the system.

5) Although improved performance as compared with systems without the software limiters can be expected, no guarantees of closed-loop stability can be made.

Acknowledgments

This research was supported by NASA Grant NAG1-1744 from NASA Langley Research Center. The Technical Manager was Barton Bacon.

References

[1]Snell, S. A., Enns, D. F., and Garrard, W. L., Jr., "Nonlinear Inversion Flight Control for a Supermaneuverable Aircraft," *Journal of Guidance, Control, and Dynamics*, Vol. 15, No. 4, 1992, pp. 976–984.

[2]Powers, B. G., "Space Shuttle Longitudinal Landing Flying Qualities," *Journal of Guidance, Control, and Dynamics*, Vol. 9, No. 5, 1986, pp. 566–572.

[3]Dornheim, M. A., "Report Pinpoints Factors Leading to YF-22 Crash," *Aviation Week and Space Technology*, Nov. 1992, pp. 53, 54.

[4]Anon., "Why the Gripen Crashed," *Aerospace America*, Vol. 32, No. 2, 1994, p. 11.

[5]McKay, K., "Summary of an AGARD Workshop on Pilot Induced Oscillation," AIAA Paper 94-3668, Aug. 1994.

[6]Bryson, A. E., Jr., and Ho, Y. C., *Applied Optimal Control*, Hemisphere, New York, 1989.

[7]Kothare, M. V., Campo, P. J., Morari, M., and Nett, C. N., "A Unified Framework for the Study of Anti-Windup Designs," *Automatica*, Vol. 30, No. 12, 1994, pp. 1869–1883.

[8]Kapasouris, P., Athans, M., and Stein, G., "Design of Feedback Control Systems for Unstable Plants with Saturating Actuators," *IFAC Symposium on Nonlinear Control Systems Design* (Capri, Italy), edited by A. Isidori, Pergamon, Oxford, England, UK, 1989, pp. 302–307.

[9]Mayne, D. Q., and Schroeder, W. R., "Nonlinear Control of Constrained Linear Systems," *International Journal of Control*, Vol. 60, No. 5, 1994, pp. 1035–1043.

[10]Horowitz, I., "A Synthesis Theory for a Class of Saturating Systems," *International Journal of Control*, Vol. 38, No. 1, 1983, pp. 169–187.

[11]A'Harrah, R. C., "An Alternate Control Scheme for Alleviating Aircraft-Pilot Coupling," AIAA Paper 94-3673, Aug. 1994.

[12]Nise, N. S., *Control Systems Engineering*, 1st ed., Benjamin/Cummings, Redwood City, CA, 1992, p. 324.

[13]Adams, R. J., Buffington, J. M., Sparks, A. G., and Banda, S. S., "An Introduction to Multivariable Flight Control System Design," Flight Dynamics Directorate, WL-TR-92-3110, Wright–Patterson AFB, OH, 1992.

[14]Klyde, D. H., Aponso, B. L., Mitchell, D. G., and Hoh, R. H., "Development of Roll Attitude Quickness Criteria for Fighter Aircraft," AIAA Paper 95-3205, Aug. 1995.

[15]Smith, R. E., and Sarrafian, S. K., "Effect of Time Delay on Flying Qualities: An Update," *Journal of Guidance, Control, and Dynamics*, Vol. 9, No. 5, 1986, pp. 578–584.